Postprint of: Jakubowska B., Mikielewicz D., Klugmann M., Experimental study and comparison with predictive methods for flow boiling heat transfer coefficient of HFE7000, International Journal of Heat and Mass Transfer, Vol. 142 (2019), 118307, DOI: 10.1016/j.ijheatmasstransfer.2019.06.063

Experimental study and comparison with predictive methods for flow boiling heat transfer coefficient of HFE7000

Blanka Jakubowska[1], Dariusz Mikielewicz, Michał Klugmann

Gdansk University of Technology, Faculty of Mechanical Engineering, Department of Energy and Industrial Apparatus, ul. Narutowicza 11/12, 80-233 Gdansk, Poland

[1]corresponding author: blanka.jakubowska@pg.edu.pl

ABSTRACT

This article describes an experimental study of flow boiling of HFE7000 inside a smooth vertical channel. The investigation has been carried out in a circular stainless-steel tube with an inner diameter of 2.3 mm. The data have been collected for the applied heat fluxes q ranging from 61 to 205 kW/m^2, the mass flux G ranging from 214 to 1006 kg/(m^2·s), the saturation temperature T_{sat} ranging from 30 to 54°C and the full range of vapour quality x. The collected experimental data base amounted to 1,217 experimental points. The acquired results indicated that heat flux and saturation temperature have the most significant impact on the heat transfer coefficient. The local heat transfer coefficient increases with both the heat flux and saturation temperature, while the mass flux did not exhibit a significant effect on the variation of the heat transfer coefficient. The present experimental data have been compared with various heat transfer correlations from literature including the recently enhanced in-house model. The results of comparisons indicated the superiority of the in-house model over other correlations.

Keywords:

flow boiling; heat transfer coefficient; synthetic refrigerants; minichannels

NOMENCLATURE

Bo	–	boiling number (-)
C	–	mass concentration of droplets in two-phase core (-)
Co	–	convection number (-)
Con	–	confinement number (-)
c_p	–	specific heat (J/(kg·K))
d	–	diameter (m)
f, f_r	–	friction factor (-)
Fr	–	Froude number (-)

f_1, f_{1z} – function (-)

G – mass flux (kg/(m^2·s))

GWP – Global Warming Potential (-)

M – molar mass (kg/kmol)

MAD – mean absolute deviation (%)

ODP – Ozone Depletion Potential (-)

P – electrical power (W)

p – pressure (Pa)

Pr – Prandtl number (-)

q – heat flux (W/m^2)

Re – Reynolds number (-)

T – temperature (^{o}C)

We – Weber number (-)

x – quality (-)

X – Martinelli parameter (-)

Greek symbols

α – heat transfer coefficient (W/(m^2·K))

σ – surface tension (N/m)

λ – thermal conductivity (W/(m·K))

ρ – density (kg/m^3)

μ – dynamic viscosity (Pa·s)

ϕ_{LO}^2 – two-phase multiplier (-)

Subscripts

crit – critical

exp – experimental

g – vapour

h – hydraulic

l – liquid

LO – total liquid flow rate

Pb – pool boiling

r – reduced

sat – saturation

TP – two-phase

TBP – two-phase boiling

th – theoretical

1. Introduction

The literature reports that scientists from different countries have carried out research on phase change since the 17th centuries. Oliver Evans [1] was the first, who suggested using a volatile fluid in a closed cycle to freeze water. In 1828 Jacob Perkins and Richard Trevithick proposed an air-cycle system for refrigeration. Unfortunately, both systems have not been made [2]. However, in 1824 Perkins [3] constructed and patented a device using a volatile fluid for the purpose of producing the cooling and freezing. Despite the fact that this device used sulfuric ether as the refrigerant, many refrigeration experts recognize this achievement as a significant contribution to the identification of phase change mechanisms [2].

Solvents and other available volatile fluids, which are flammable and toxic in most cases, were commonly used refrigerants at the beginning of their use. Around 1930, commercial production of refrigerants belonging to the group of chlorofluorocarbons (CFCs) and hydrochlorofluorocarbons (HCFCs) had begun [4,5], which later found application for example in small refrigeration, air-conditioning and heat pumps.

Based on the Vienna Convention for the Protection of the Ozone Layer [6] and the later Montreal Protocol [7], as well as the Kyoto Protocol [8], refrigerants can be classified as those:

- having a strong ozone-depleting effect and a significant strengthening of the greenhouse effect (chlorofluorocarbons - CFCs),
- having a reduced effect on the ozone layer and with the moderate strengthening of the greenhouse effect (hydrochlorofluorocarbons - HCFC),
- harmless to the ozone layer and with little effect on the greenhouse effect (hydrofluorocarbons - HFC),
- harmless to the ozone layer and very little or no effect on the greenhouse effect (carbon dioxide - CO_2 (R744), natural hydrocarbons (HCs), ammonia - NH_3 (R717)).

The need for research on new working fluids enforces the fact that today's challenge of environmental responsibility requires that a substance which depletes the ozone layer or contributes to global warming must be restricted or substituted [9]. Hydrofluorocarbons were regarded as a promising alternative to CFCs [10]. Unfortunately, one of the most popular hydrofluorocarbons (HFC), namely R134a, has a 100-year Global Warming Potential (*GWP*) equal to 1430 in low to medium evaporation temperatures [11]. Therefore, it must be replaced by

more environmentally friendly refrigerants in the near future. Consequently, a long-term alternative to withdrawn refrigerants must be searched. For this reason, synthetic working fluids, which belong to a relatively new group of refrigerants (HFO) and characterized by a low potential of the greenhouse effect, are becoming more popular. R1234yf and R1234ze have been believed to be a promising candidate as an alternative for R134a [12]. In the case of R1234yf, its *ODP* is equal to 0, whereas the *GWP* = 4 and its thermophysical properties are similar to those of R134a. The differences in heat transfer coefficients for those refrigerants is very small, both from the low to the high vapour quality region [13]. Also, Del Col et al. [14] found that there were no significant differences between the flow boiling performance of R1234yf and R134a. Mikielewicz et al. collected experimental data from various past studies and presented the results of calculations performed using the authors' model [15,16] to predict the heat transfer coefficient during flow boiling for refrigerants R134a and R1234yf [17]. Some studies have considered a natural refrigerants namely carbon dioxide [18,19] as possible replacements for R134a, for example in air conditioning or refrigeration or Organic Rankine Cycle (ORC) systems. Carbon dioxide compared to other working fluids is relatively safe, is non-toxic, non-flammable, non-explosive, inexpensive and can be coupled with most metals and plastics [20]. On the other hand, for the carbon dioxide systems, the working pressure is significantly higher than for R134a systems, which would lead to significant modifications and higher costs [21]. In that light, hydrofluoroethers (HFE), which exhibit a lower impact on the environment, are also regarded as promising alternatives to CFCs [22], and under consideration in many areas of potential application. It should be added that most fluorinated, especially HFEs possess zero ozone depletion potential (*ODP*), low global warming potentials (*GWP*) and relatively short atmospheric lifetimes (*ALT*). In addition, most HFEs exhibit low toxicity, are non-flammable and thermally stable and thus have excellent environmental compatibility [9,23]. In the present work, HFE7000 has been selected for scrutiny. The selected thermophysical properties of HFE7000 are shown in Table 1. It should also be noted that this working fluid is non-flammable, of low toxicity and non-corrosive. Furthermore, it is characterised by a zero *ODP* and a *GWP* is equal to 530 [24]. A lot of traditional applications such as cooling devices, food refrigeration, industrial cooling and thermal management of semiconductors may become a potential area for application of HFE7000 [25].

Table 1. The selected thermophysical properties of HFE7000 [9,26]**.**

T_{sat}, °C	P_{sat}, kPa	ρ_l, kg/m^3	ρ_g, kg/m^3	h_l, kJ/kg	h_g, kJ/kg	σ, kN/m
0	22.940	1470.5	2.0552	200.00	351.88	14.39299
20	57.072	1418.0	4.8461	225.08	368.29	12.28273
30	85.052	1390.5	7.0676	237.80	376.59	11.24976
40	122.78	1362.2	10.023	250.68	384.93	10.2329
50	172.35	1332.7	13.876	263.72	393.27	9.23332
60	235.99	1301.9	18.821	276.93	401.60	8.252382

Nowadays, there is still observed rapid development of practical engineering applications for micro-devices, micro-systems, compact heat exchangers and highly integrated cooling systems [25,27,28]. Therefore, the aims are to a better understanding and improving the knowledge of small and micro-scale heat transfer phenomena. In addition, in order to obtain a high value of heat transfer coefficient, the single-phase heat transfer is not enough. Hence, the activities have been taken to replace devices using single-phase heat transfer by their alternatives using boiling or condensation. Taking into consideration, the complexity of these phenomena and a general trend towards using the new environmentally friendly working fluids, which also require validated tools that are able to predict the pressure drop and heat transfer coefficient, there is a need to increase the accuracy of modelling boiling and condensation phenomena.

In the literature, there are still not enough experimental data for flow boiling and condensation conducted for HFEs. Mikielewicz et al. [25] have presented their experimental results of the pressure drop of HFE7000 and HFE7100 during flow condensation in minichannels. In this case, the flow was examined in a cylindrical single channel with a 2.3 mm inner diameter. Additionally, the experimental data, which they obtained, were compared with some well-established correlations for pressure drop during two-phase flow. That comparison resulted in a conclusion that the correlation due to Fronk and Garimella [29] and the in-house model for flow boiling and flow condensation [30] were found to be in best agreement with the experimental data. Forced convective boiling experiments with HFE7000 as the working fluid were conducted for upward flow in a vertical tube at 122 kPa and mass flux ranging between 50 and 150 kg/(m^2·s) by Eraghubi et al. [31]. The experimental facility consisted of a smooth tube with an inside diameter of 8 mm and an overall length of 120 mm. The results obtained by Eraghubi et al. [31] show that after the onset of nucleate boiling, the flow regime is bubbly and increasing the heat flux acts to increase the boiling heat transfer coefficient due to in-

creased nucleation site density, bubble frequency and size. In the article [31], the convective boiling heat transfer correlation due to Chen [32] was compared with the measured data showing a reasonable agreement and Eraghubi et al. [31] proposed a modified Chen correlation for the low mass flux convective boiling, which turned out to be superior to the original model.

On the basis of the above, the authors decided to test HFE7000 working fluid for flow boiling in a vertical tube. Additionally, the comparison of experimental heat transfer during the flow boiling of HFE7000 with the calculation results using selected predictive methods has also been presented in the paper.

2. Experimental facility

As a part of studies that are presented in this article, an experimental facility, which was constructed for previous research [25], was modified and used in order to the examination of flow boiling in vertical channels. It is worth mentioning that this experimental facility was designed as a compact and mobile installation with dimensions of 1 x 1.5 x 2 m. A schematic of the facility is presented in Figure 1.

In the presented facility the test of simultaneous process of both cases, namely flow boiling and flow condensation with any low boiling point fluid with the heat of vaporisation not exceeding 200 kJ/kg and installation pressure below 10 bar can be conducted [25]. Working fluid circulation is forced by an electrically-driven pump. The selected gear pump provides the circulation of fluid in the test section without any pulsation. Adjustment of the mass flow rate can be realised by changing the voltage of the pump's power supply or using the by-pass [25]. Firstly, the working fluid from the main tank, made of stainless steel and a maximum capacity of 21 dm^3, is pumped to the Danfoss Coriolis type mass flowmeter MASS D1 3 working with the MASS 6000 19" IP20 interface. The measuring range of this mass flowmeter is 0 – 65 kg/h at the temperature range of working fluid -50 – 125 ^oC. Before the working fluid is entered into the evaporation section the required inlet parameters must be achieved in the pre-heater. When the working fluid reaches the evaporation section, its heating is realised in a vertical silver tube of 2.3 mm inner diameter and length 24 cm in the flow boiling part of the facility, powered by a low voltage, high current DC power supply [25]. It is possible to obtain a full range of quality x variation as well as superheating about 1 – 2 K. In order to determine the heat flux and quality, current, voltage, inlet and outlet temperatures and pressures are measured. The distribution of tube wall temperature is registered using the infrared camera FLIR A325, operating in Researcher Pro 2.9 software (Figure 2). An example of the

wall temperature distribution depending on the distance from the beginning of the heating section is presented in Figure 3. In order to measure the wall temperature, the test section visible in the thermovision image between markers of 20 cm length, was divided into 100 equally spaced sections. Inlet temperature and pressure, as well as outlet temperature and pressure, are also measured. The pressure is monitored by an absolute pressure transducer (Keller PAA-33X, measurement range 0–3 bar). The uncertainty analysis of the operating parameters is presented in Table 2. All tests were performed under steady-state conditions. The temperature, mass flow and system pressure were recorded using a data logger connected to a computer.

Table 2. Uncertainty of measurements.

Measured quantity/instrument	Uncertainty
Mass flux of working fluid, kg/s	$\pm$0.125
Heat flux, W	$\pm$4.7
Temperature –K type thermocouple, K	$\pm$0.3
Wall temperature, K	$\pm$2.5
Pressure – Keller PAA-33X, bar	$\pm$0.00108

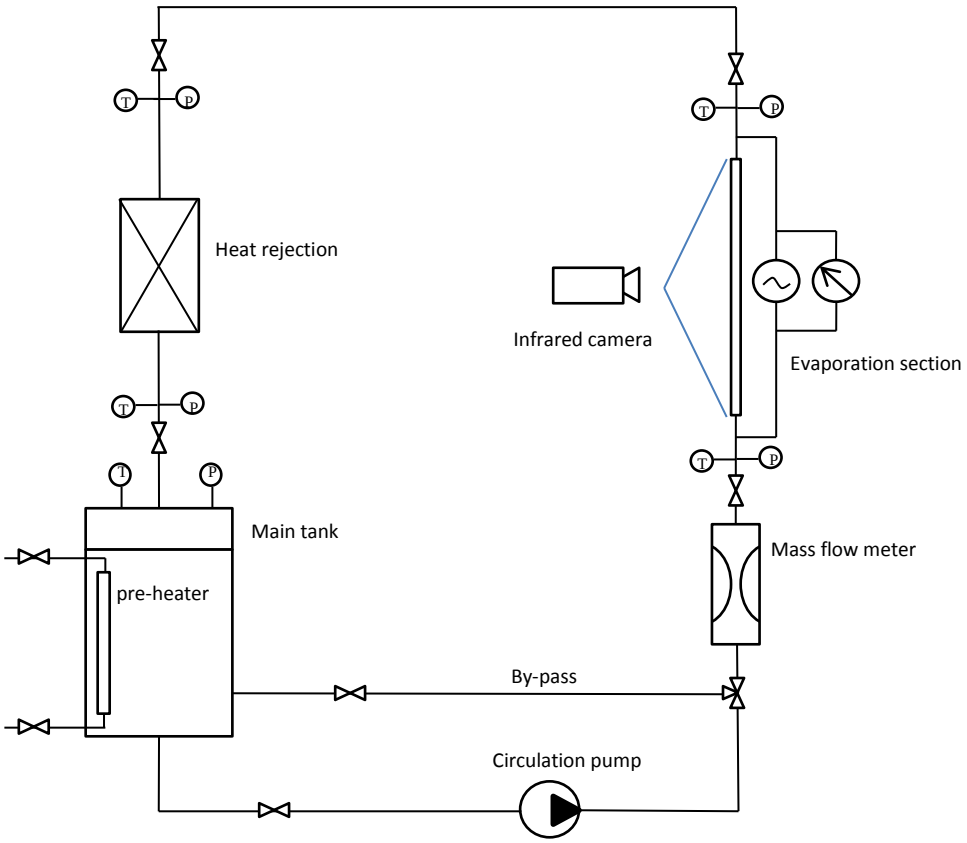

Figure 1. Schematic diagram of the experimental facility.

3. Data reduction

The value of the local heat transfer coefficient α was calculated using the relationship resulting from the heat balance equation applied to the test section:

$$P = \alpha \cdot A \cdot \Delta T \tag{1}$$

where P is electrical power, A – surface associated with the inner wall, ΔT – local temperature differences between wall temperature and fluid temperature. The heat balance was also calculated from the heat balance on the fluid inside the test section using the following equation:

$$P = \dot{m} \cdot \left(h_{out} - h_{in}\right) \tag{2}$$

where $\dot{m}$ is measured mass flow rate, h_{out} and h_{in} are the outlet and inlet enthalpies to the test section determined using the Refprop9 database [26].

In calculations, the local wall temperatures were directly measured by the infrared camera. A sample image obtained from the infrared camera, which registered the distribution of tube wall temperature, is shown in Figure 2, where the fluid temperature was determined from the

local saturation temperature, which was also determined using the Refprop9 database [26] and defined based on the local measured pressure. While, the thermodynamic vapour quality for distance from the inlet *z*, was determined from the following heat balance equation:

$$x = \frac{h_z - h_l}{h_g - h_l} \tag{3}$$

where h_z is the value of the local total enthalpy at a distance of z from the beginning of the section, whereas h_l and h_g are the saturated values of the liquid and vapour enthalpies corresponding to the local pressure.

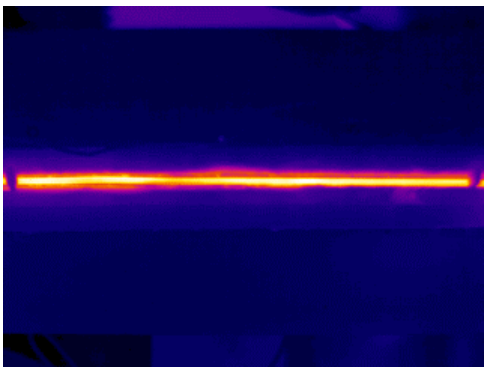

Figure 2. The distribution of tube wall temperature using the infrared camera.

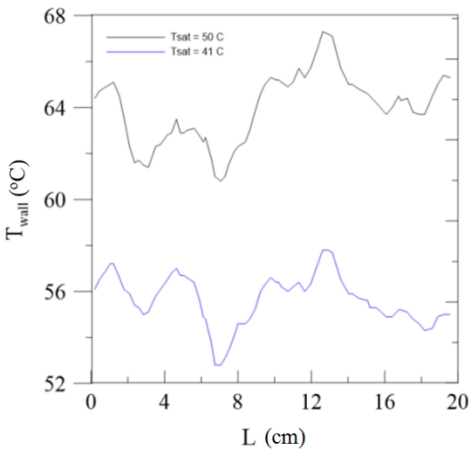

Figure 3. The change of the wall temperature for example saturation temperatures.

The total enthalpy h_z was calculated using the following equation:

$$h_z = h_{in} + \frac{P \cdot U \cdot z}{A \cdot \dot{m}} \tag{4}$$

From the knowledge of the saturation temperature of working fluid T_{sat}, wall temperature T_{wall} and heat flux q, it was possible to determine the local value of the heat transfer coefficient α_z., which can be evaluated as the ratio of the heat flux to saturation minus the inside wall temperature:

$$\alpha_z = \frac{q}{(T_{wall} - T_{sat})} \tag{5}$$

The sequential perturbation method [33], which was used to determination of experimental uncertainty, allows estimation of the total experimental error. Determination of the total error using this method is possible by taking into account errors form individual sources in a general database and averaging them using a root sum square method (RSS). This method of er-

ror analysis was carried out for each of data measurements series. Besides, the heat balance was tested for each series and in the case of flow boiling, it was based on the enthalpy difference. On the basis of conducted error analysis, it was found that the average uncertainty of heat transfer coefficient determination did not exceed 5%. Details are presented in Table 3.

Table 3. Partial experimental uncertainties.

Parameter	Operating range	Uncertainty
d, mm	2.3	±0.007 mm
G, kg/(m^2·s)	214–1006	± 0.3%
q, kW/(m^2·K)	61–205	± 3.5%
T_{sat}, °C	30–54	± 0.1%
α_{exp} kW/(m^2·K)	3.45–15.72	± 5%
x, (-)	0–1	± 4%

4. Experimental results and discussion

The effects of mass flux on the heat transfer coefficient of HFE7000 have been presented in Figures 4 to 7, which show the distribution for selected flow parameters of the heat transfer coefficient during flow boiling of HFE7000 as a function of vapour quality at different mass fluxes and constant saturation temperature and heat flux.

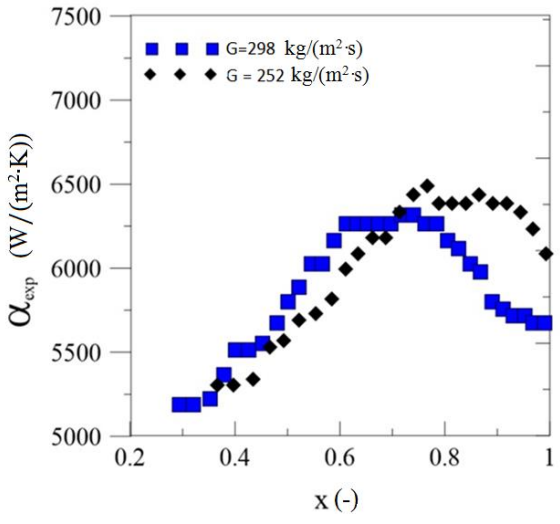

Figure 4. Heat transfer coefficient versus vapour quality of 2.3 mm horizontal tube at T_{sat} = 33°C and q = 78 kW·m^{-2}·K^{-1} during flow boiling of HFE7000.

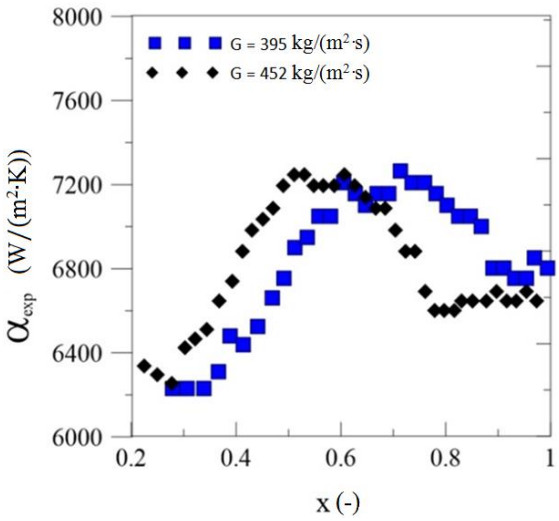

Figure 5. Heat transfer coefficient versus vapour quality of 2.3 mm horizontal tube at T_{sat} = 37°C and q = 96 kW·m^{-2}·K^{-1} during flow boiling of HFE7000.

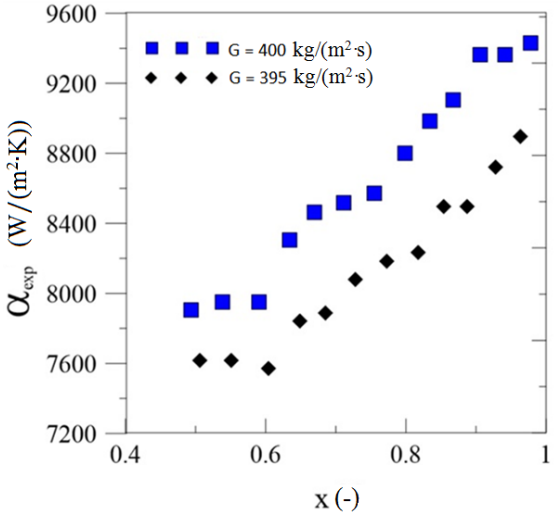

Figure 6. Heat transfer coefficient versus vapour quality of 2.3 mm horizontal tube at T_{sat} = 40°C and q = 132 kW/(m^2·K) during flow boiling of HFE7000.

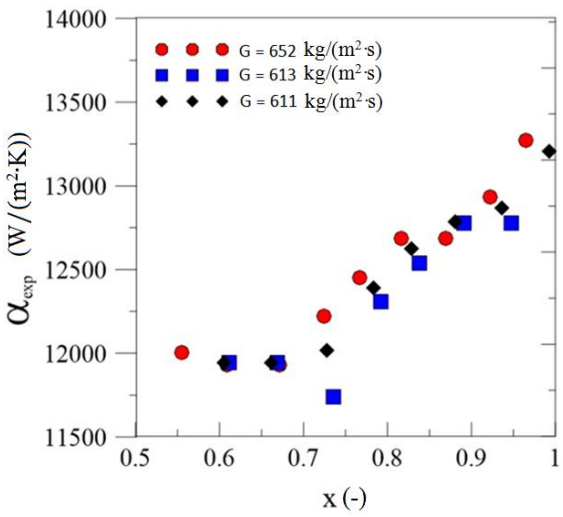

Figure 7. Heat transfer coefficient versus vapour quality of 2.3 mm horizontal tube at T_{sat} = 50°C and q = 200 kW/(m^2·K) during flow boiling of HFE7000.

According to the presented results, it can be seen that the value of heat flux has a strong influence on heat transfer coefficients (HTC), with no significant effect from mass flux values. HTCs, initially, slightly decrease with vapour quality in the low-quality region (x<0.3) and then increase with a further increase in vapour quality. The decreasing trend of heat transfer coefficients in the low-quality region has been also observed by Del Col et al. [14]. Furthermore, the increase in the value of heat transfer coefficients has been obtained by the increase in saturation temperature. Moreover, at low mass flux, the vapour quality does not have a significant impact on heat transfer coefficients. For example, in the case presented in Figures 4 and 5, the heat transfer coefficient increased to about 1 kW/(m^2·K). However, heat transfer coefficients increased more with vapour quality at higher mass flux conditions. Similar observations in research have been noticed by Coppeti et al. [34]. Furthermore, increasing the mass flux with the same heat flux and saturation temperature values does not cause a significant increase in heat transfer coefficients. Summarising, the value of heat transfer coefficients during flow boiling of HFE7000 is strongly affected by heat flux and saturation temperature with negligible effects from the mass flux and vapour quality.

Next, the experimental results have been compared with selected correlations from the literature. For this purpose, 16 correlations have been selected and are presented in Table 4.

Table 4. Selected correlations describing heat transfer coefficient during flow boiling.

Authors	Equations	Remarks	Details of the nomenclature
For conventional channels			
Fang et al. [35]	$Nu = F_f \cdot M^{-0.8} \cdot Bo^{0.98} \cdot Fr_{LO}^{0.48} \cdot Bd^{0.72} \cdot \left(\frac{\rho_l}{\rho_g}\right)^{0.29} \cdot \left[\ln\left(\frac{\mu_{lf}}{\mu_{lw}}\right)\right]^{-1} \cdot Y$ (6) $Y = \begin{cases} 1 & \text{for } p_r \le 0.43 \\ 1.38 - p_r^{1.15} & \text{for } p_r > 0.43 \end{cases}$ (7)	based on two experimental databases: 1° 17,778 experimental points for 13 refigerants 2° 6,664 experimental points for 18 refigerants	*Nu* – Nusselt number (-) *M* – molar mass (kg/kmol) μ_{lf} – dynamic viscosity for fluid temperature (Pa·s) μ_{lw} – dynamic viscosity for wall temperature (Pa·s) ρ – density (kg/m^3) p_r – reduced pressure (-) F_f – constant depending on the type of workin fluid (-) Fr_{LO} – Froude number (-) $Fr_{LO} = \frac{G^2}{g \cdot d_h \cdot \rho_l^2}$ *Bo* – boiling number (-) $Bo = \frac{q}{G \cdot h_{l,g}}$ *Bd* – Bond number (-) $Bd = \frac{g \cdot (\rho_l - \rho_g) \cdot d_h^{\,2}}{\sigma}$
Chen [32]	$\alpha_{TPB} = S \cdot \alpha_{Pb} + F \cdot \alpha_{LO}$ (8)	over 600 experimental points for water and organic refrigerants	α_{Pb} – pool boiling heat transfer coefficient (W/(m^{2}K)) α_{LO} – heat transfer coefficient for the liquid phase (W/(m^{2}K)) *S*– suppressing factor (-)

			F– enhacement factor (-)
Bertsch et al. [36]	$\alpha_{TPB} = (1-x)\cdot\alpha_{Pb} + \left[1+80\cdot\left(x^2-x^6\right)\cdot e^{-0.6\cdot Con}\right]\cdot\alpha_{LO}$ (9)	based on 3,899 experimental points for 12 refrigerants from literature	α_{Pb} – pool boiling heat transfer coefficient (W/(m^{2}K)) x– vapour quality (-) α_{LO} – heat transfer coefficient for the liquid phase (W/(m^{2}K)) Con – confinement number (-)
Shah [37]	$\alpha_{TPB} = F\cdot\alpha_{LO}$ (10) $F = \max(F_{CB}, F_{NB})$ (11)	based on 800 experimental points	α_{LO} – heat transfer coefficient for the liquid phase (W/(m^{2}K)) F– enhacement factor (-) F_{CB}, F_{NB} – function (-)
Gungor and Winterton [38]	$\alpha_{TPB} = S\cdot\alpha_{Pb} + F\cdot\alpha_{LO}$ (12) $F = 1+24000\cdot Bo^{1.16}+1.37\cdot\left(\frac{1}{X}\right)^{0.86}$ (13) $S = \left[1+1.15\cdot10^{-6}\cdot F^2\cdot \mathrm{Re}_l^{1.17}\right]^{-1}$ (14)	based on 3,693 experimental points from literature, modification of Chen correlation	S– suppressing factor (-) F– enhacement factor (-) F_{new}– modified enhacement factor (-) α_{Pb} – pool boiling heat transfer coefficient (W/(m^{2}K)) α_{LO} – heat transfer coefficient for the liquid phase (W/(m^{2}K)) Bo – boiling number (-) X – Martinelli parameter (-) x– vapour quality (-) ρ – density (kg/m^3)
Gungor and Winterton [39]	$\alpha_{TPB} = F_{new}\cdot\alpha_{LO}$ (15) $F_{new} = 1+3000\cdot Bo^{0.86}+1.12\cdot\left(\frac{x}{1-x}\right)^{0.75}\cdot\left(\frac{\rho_l}{\rho_g}\right)^{0.41}$ (16)	a simpler version of the correlation	

			Re_l– Reynolds number (-) $\mathrm{Re}_l = \frac{(1-x)\cdot G\cdot d_h}{\mu_l}$
Kim and Mudawar [40]	$\alpha_{TPB} = \left(\alpha_{Pb}^2 + \alpha_{LO}^2\right)^{\frac{1}{2}}$ (17) $\alpha_{Pb} = \left[2345\cdot\left(Bo\cdot\frac{P_H}{P_F}\right)^{0.7}\cdot p_r^{0.38}\cdot(1-x)^{-0.51}\right]\cdot\left(0.023\cdot\mathrm{Re}_l^{0.8}\cdot\mathrm{Pr}_l^{0.4}\cdot\frac{\lambda_l}{d_h}\right)$ (18) $\alpha_{LO} = \left[5.2\cdot\left(Bo\cdot\frac{P_H}{P_F}\right)^{0.08}\cdot We_l^{-0.54}\cdot 3.5\cdot\left(\frac{1}{X}\right)^{0.94}\cdot\left(\frac{\rho_g}{\rho_l}\right)^{0.25}\right]\cdot\left(0.023\cdot\mathrm{Re}_l^{0.8}\cdot\mathrm{Pr}_l^{0.4}\cdot\frac{\lambda_l}{d_h}\right)$ (19)	based on 10,805 experimental points from literature for 18 refrigerants	α_{Pb} – pool boiling heat transfer coefficient (W/(m^{2}K)) α_{LO} – heat transfer coefficient for the liquid phase (W/(m^{2}K)) p_r – reduced pressure (-) d_h – diameter (m) λ – thermal conductivity (W/(mK)) ρ – density (kg/m^3) P_H – heat perimeter (m) P_F – wetted perimeter (m) Bo – boiling number (-) We_l – Weber number (-) $We_l = \frac{G^2\cdot d_h}{\rho_l\cdot\sigma}$ X – Martinelli parameter (-) x– vapour quality (-) Pr –Prandtl number (-) Re_l– Reynolds number (-)
Wojtan et al. [41]	$\alpha_{TPB} = \frac{\Theta_{dry}\cdot\alpha_g + (2\pi - \Theta_{dry})\cdot\alpha_{wet}}{2\pi}$ (20) $\alpha_g = 0.023\cdot\mathrm{Re}_g^{0.8}\cdot\mathrm{Pr}_g^{0.4}\cdot\frac{\lambda_g}{d_h}$ (21)	based on over 1250 eperimental points, R22, R410A, G = 70 – 700 kg/(m^{2}s), q= 2 – 57.5 kW/m^2, low saturation temparature	Θ_{dry} – dry angle (rad) α_g – heat transfer coefficient for the dry perimeter (W/(m^{2}K))

	$\alpha_{wet} = \left(\alpha_{cb}^3 + \alpha_{Pb}^3\right)^{\frac{1}{3}}$ (22) $\alpha_{cb} = 0.0133 \cdot \mathrm{Re}_{\delta}^{0.69} \cdot \mathrm{Pr}_l^{0.4} \cdot \frac{\lambda_l}{\delta}$ (23) $\alpha_{Pb} = 0.8 \cdot 55 \cdot p_r^{0.12} \cdot M^{-0.5} \cdot \left(-\log p_r\right)^{-0.55} \cdot q^{0.67}$ (24)		α_{wet} – heat transfer coefficient for the wet perimeter (W/(m^{2}K)) α_{cb} – convective boiling heat transfer coefficient (W/(m^{2}K)) δ – liquid film thickness (m) q – heat flux (W/m^2) p_r – reduced pressure (-) d_h – diameter (m) λ – thermal conductivity (W/(mK)) Re_δ – liquid film Reynolds number (-) $\mathrm{Re}_\delta = \frac{4 \cdot G \cdot \delta \cdot (1-x)}{\mu_l \cdot (1-\varepsilon)}$ Re_g – Reynolds number (-) $\mathrm{Re}_g = \frac{G \cdot x \cdot d_h}{\mu_g \cdot \varepsilon}$ ε – cross-sectional vapor void fraction (-) *(new)* – modified value (-)
Lillo et al. [42]	$\alpha_{TPB} = \frac{\Theta_{dry} \cdot \alpha_g + \left(2\pi - \Theta_{dry}\right) \cdot \alpha_{wet(new)}}{2\pi}$ (25) $\alpha_{wet(new)} = \left(\alpha_{cb(new)}^3 + \alpha_{Pb(new)}^3\right)^{\frac{1}{3}}$ (26) $\alpha_{cb(new)} = 0.5 \cdot \alpha_{cb}$ (27) $\alpha_{Pb(new)} = 1.7 \cdot \alpha_{Pb}$ (28)	d_h = 6mm, G = 150 – 500 kg/(m^{2}s), q = 2.5 – 40 kW/m^2, Tsat = 25 – 35^{o}C, R290, modification of Wojtan et al. correlation	
For minichannels			
Lazarek and Black [43]	$\alpha_{TPB} = \left(30 \cdot \mathrm{Re}_{LO}^{0.857} \cdot Bo^{0.714}\right) \cdot \frac{\lambda_l}{d_h}$ (29)	d = 3.15 mm, R113	Bo – boiling number (-) Re_{LO} – Reynolds number (-) d_h – diameter (m) λ – thermal conductivity (W/(mK))

			$\mathrm{Re}_{LO} = \frac{G \cdot d_h}{\mu_l}$
Li and Wu [44]	$\alpha_{TPB} = 334 \cdot Bo^{0.3} \cdot \left(Bd \cdot \mathrm{Re}_l^{0.36}\right)^{0.4} \cdot \frac{\lambda_l}{d_h}$ (30)	d_h = 0.16 – 3.1 mm, water, FC77	d_h – diameter (m) λ – thermal conductivity Bo – boiling number (-) Re_l– Reynolds number (-) Bd – Bond number (-)
Docoulombier et al. [45]	$\alpha_{TPB} = \max(\alpha_{Pb}, \alpha_{LO})$ (31) $\alpha_{LO} = \left[1.47 \cdot 10^4 \cdot Bo + 0.93 \cdot \left(\frac{1}{X}\right)^{\frac{2}{3}}\right] \cdot \left(0.023 \cdot \mathrm{Re}_{LO}^{0.8} \cdot \mathrm{Pr}_l^{1/3} \cdot \frac{\lambda_l}{d_h}\right)$ if $Bo > 1.1 \cdot 10^{-4}$ (32) $\alpha_{LO} = \left[1 + 1.8 \cdot \left(\frac{1}{X}\right)^{0.986}\right] \cdot \left(0.023 \cdot \mathrm{Re}_{LO}^{0.8} \cdot \mathrm{Pr}_l^{0.4} \cdot \frac{\lambda_l}{d_h}\right)$ if $Bo < 1.1 \cdot 10^{-4}$ (32) $\alpha_{Pb} = 131 \cdot p_r^{-0.0063} \cdot \left(-\lg p_r\right)^{-0.55} \cdot M^{-0.5} \cdot q^{0.58}$ (33)	d = 0.16–3.1 mm, water, FC77, ethanol, propane, CO_2, 3,744 experimental points	α_{Pb} – pool boiling heat transfer coefficient (W/(m^{2}K)) α_{LO} – heat transfer coefficient for the liquid phase (W/(m^{2}K)) d_h – diameter (m) λ – thermal conductivity (W/(mK)) Bo – boiling number (-) Re_{LO} – Reynolds number (-) X – Martinelli parameter (-) Pr –Prandtl number (-) q – heat flux (W/m^2) M – molar mass (kg/kmol) p_r – reduced pressure (-)
Lee and Mudawar [46]	$\alpha_{TPB} = 3.856 \cdot X^{0.267} \cdot \alpha_{LO}$ for 0<x<0.05 (34) $\alpha_{TPB} = 436.48 \cdot Bo^{0.522} \cdot We^{0.331} \cdot X^{0.665} \cdot \alpha_{LO}$ for 0.05<x<0.55 (35) $\alpha_{TPB} = \max\left(108.6 \cdot X^{0.665} \cdot \alpha_{LO}, \cdot \alpha_{LO}\right)$ for 0.55<x<1 (36)	flow patterns	X – Martinelli parameter (-) Bo – boiling number (-) We – Weber number (-) α_{LO} – heat transfer coefficient for the liquid phase (W/(m^{2}K))

			x– vapour quality (-)
Owhaib [47]	$\alpha_{TPB} = 400 \cdot (\mathrm{Re}_{LO} \cdot Bo)^{0.5} \cdot (1 - x_e)^{0.1} \cdot Con^{0.55} \cdot p_r^{1.341} \cdot \left(\frac{\rho_l}{\rho_g}\right)^{0.37} \cdot \frac{\lambda_l}{d_h}$ (37)	d = 1.7, 1.224, 0.826 mm, R134a	x_e– vapour quality at the outlet (-) Con – confinement number (-) Bo – boiling number (-) Re_{LO} – Reynolds number (-) p_r – reduced pressure (-) d_h – diameter (m) λ – thermal conductivity (W/(mK)) ρ – density (kg/m^3)
Mikielewicz et al. [30]	$\frac{\alpha_{TBP}}{\alpha_{LO}} = \sqrt{\left(\phi_{LO}^2\right)_{MS}^n + \frac{C}{1 + 2.53 \cdot 10^{-3} \cdot \mathrm{Re}_{LO}^{1.17} \cdot Bo^{0.6} \cdot \left[\left(\phi_{LO}^2\right)_{MS} - 1\right]^{-0.65}} \left(\frac{\alpha_{Pb}}{\alpha_{LO}}\right)^2}$ (38) $\left(\phi_{LO}^2\right)_{MS} = \left[1 + 2\left(\frac{1}{f_1} - 1\right) \cdot x \cdot Con^m\right] \cdot (1 - x)^{\frac{1}{3}} + \frac{1}{f_{1z}} \cdot x^3$ (39) $\alpha_{Pb} = 55 \cdot M^{-0.5} \cdot p_r^{0.12} \cdot (-\log p_r)^{-0.55} \cdot q^{\frac{2}{3}}$ (40)	Semi-empirical, R11, R12, R134a, R113, R123, R141b, R22	$\left(\phi_{LO}^2\right)_{MS}$ – two –phase flow multiplier Re_{LO}– Reynolds number (-) Bo – boiling number (-) Con – confinement number (-) C – mass concentration of droplets in twophase core (-) x – vapour quality (-) $p_r = \left(\frac{P_{sat}}{P_{crit}}\right)$ – reduced pressure (-) α_{LO} – heat transfer coefficient for the liquid phase (W/(m^{2}K)) α_{Pb} – pool boiling heat trans-
Mikielewicz et al. [20,48]	$\frac{\alpha_{TBP}}{\alpha_{LO}} = \sqrt{\left\{\left(\phi_{LO}^2\right)_{MS} \cdot \left[1 - \left(\frac{P_{sat}}{P_{crit}}\right)\right] + 1\right\}^n + \frac{C}{1 + \left(\frac{P_{sat}}{P_{crit}}\right)^{-0.985} \cdot 2.53 \cdot 10^{-3} \cdot \mathrm{Re}_{LO}^{1.17} \cdot Bo^{0.6} \cdot \left[\left(\phi_{LO}^2\right)_{MS} - 1\right]^{-0.65}} \left(\frac{\alpha_{Pb}}{\alpha_{LO}}\right)^2}$ (41)	based on 7,650 experimental points for 10 refrigerants: CO_2, R600a, R290, R134a, R1234yf, NH_3, R152a, R245fa, R236fa, HFE7000	

			fer coefficient (W/(m^{2}K)) q – heat flux (W/m^2) M – molar mass (kg/kmol) f_1, f_{1z} – function (-)

Due to the fact that model, which is described by equation (38), it was the original formula to the proposed modification described by equation (41) and both are the semi-empirical in-house model, more details should be given. Developed for the years the flow boiling (C = 1) and flow condensation (C = 0) correlation [49] modelling heat transfer coefficients use expression describing the two-phase flow multiplier. In both equation, namely (38) and (41), the two-phase flow multiplier is determined by using modified Müller- Steinhagen and Heck model [15], equation (39), which takes into account the influence of surface tension. The exponent n is dependent on the character of the flow, namely laminar or turbulent flow, and is respectively equal to 2 or 0.9. In equation (39), f_1 and f_{1z} are functions, which are described respectively: for turbulent flow: $f_1 = (\rho_l / \rho_g)(\mu_l / \mu_g)^{0.25}$, $f_{1z} = (\mu_g / \mu_l)(\lambda_l / \lambda_g)^{1.5}(c_{pl} / c_{pg})$, for laminar flow: $f_1 = (\rho_l / \rho_g)(\mu_l / \mu_g)$, $f_{1z} = (\lambda_g / \lambda_l)$. Whereas, exponent m is equal to 0 for flow in conventional channels and equal to -1 for flow in minichannels. It should be added, that Table 4 presents correlations describing heat transfer coefficients during flow boiling, which are dedicated to both conventional size channels and minichannels. Kew and Cornwell [50] suggested a criterion for the transition from conventional size channels to minichannels through the confinement number *Con*, defined as:

$$Con = \frac{\sqrt{\dfrac{\sigma}{g(\rho_l - \rho_g)}}}{d_h} \tag{42}$$

When the confinement number is greater than 0.5 then the flow corresponds to the flow in the minichannel. In the case of experimental research conducted for HFE7000, the confinement number varied in the range from 0.361 to 0.396, which is in accordance with the Kew and Cornwell criterion corresponding to the flow in conventional channels. Therefore, in the calculations, which were carried out, the account was taken in equation (39), m = 0. On the basis of the conducted analyses [20,48], it was found that the predictive condition of the model (38) can be enhanced by including ratio of saturation pressure to critical in both terms, convection and bubble generation.

Figures 8 to 39 present a comparison of experimental heat transfer during flow boiling of HFE7000 with the calculation results using the predictive methods listed in Table 4.

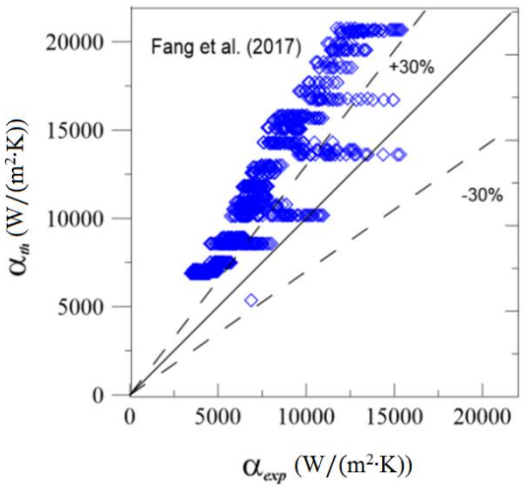

Figure 8. Comparison of the test results α_{exp} with the predictions obtained α_{th} using the Fang et al. (2017) correlation.

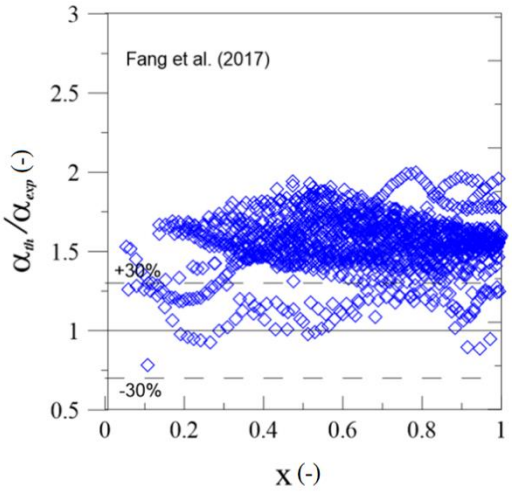

Figure 9. Comparison of the test results using the Fang et al. (2017) correlation as a function of vapour quality.

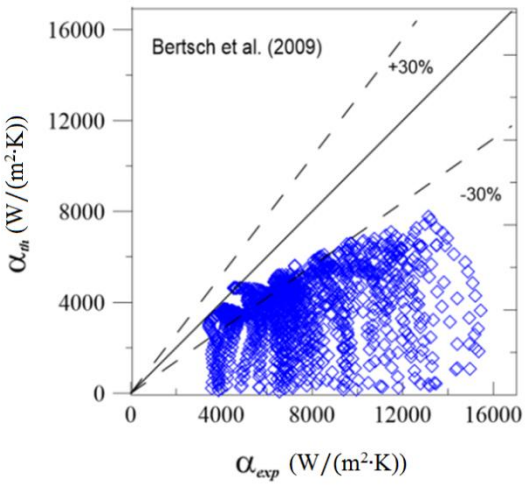

Figure 10. Comparison of the test results α_{exp} with the predictions obtained α_{th} using the Bertsch et al. (2009) correlation.

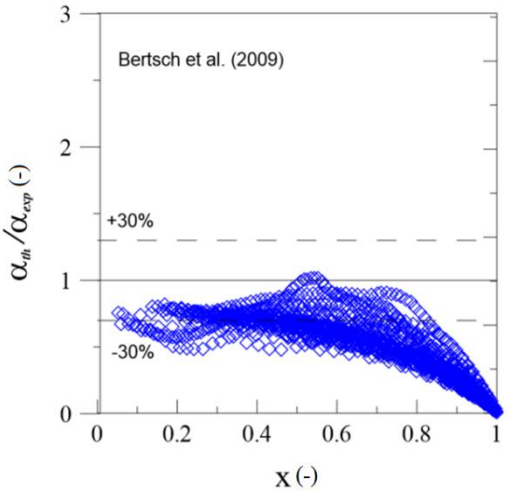

Figure 11. Comparison of the test results using the Bertsch et al. (2009) correlation as a function of vapour quality.

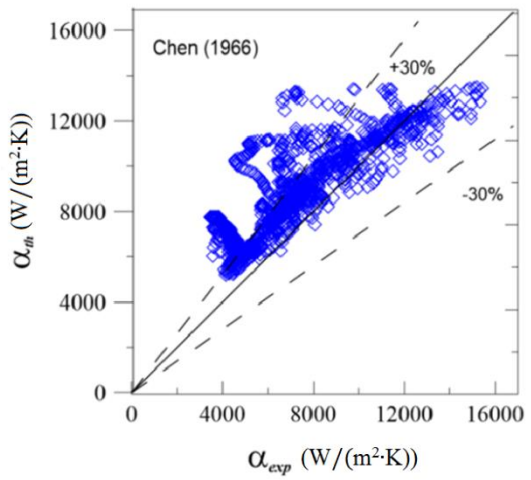

Figure 12. Comparison of the test results α_{exp} with predictions obtained α_{th} using the Chen (1966) correlation.

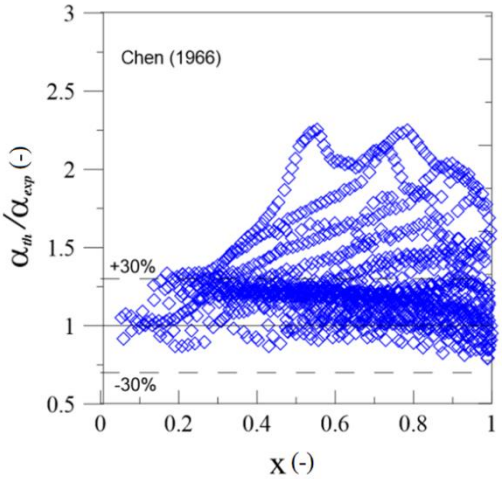

Figure 13. Comparison of the test results using the Chen (1966) correlation as a function of vapour quality.

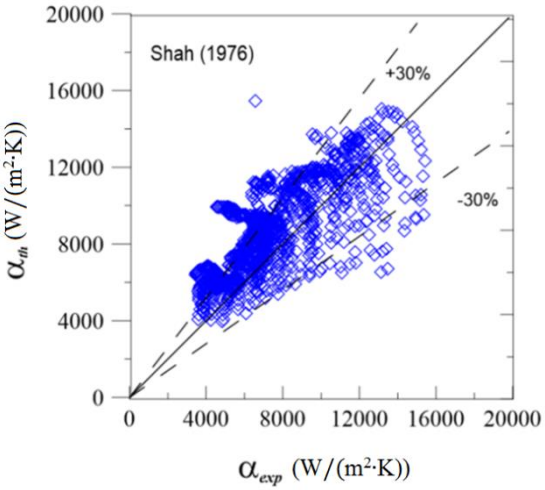

Figure 14. Comparison of the test results α_{exp} with predictions obtained α_{th} using the Shah (1976) correlation.

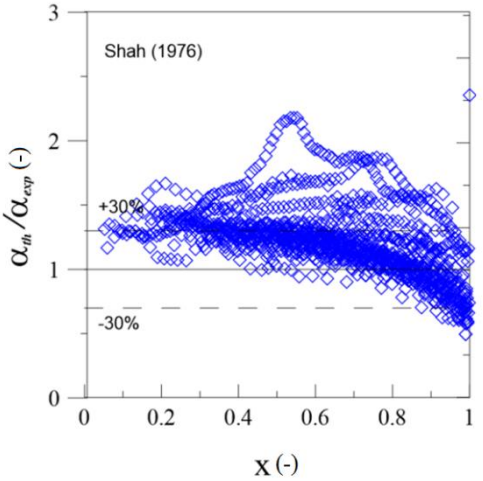

Figure 15. Comparison of the test results using the Shah (1976) correlation as a function of vapour quality.

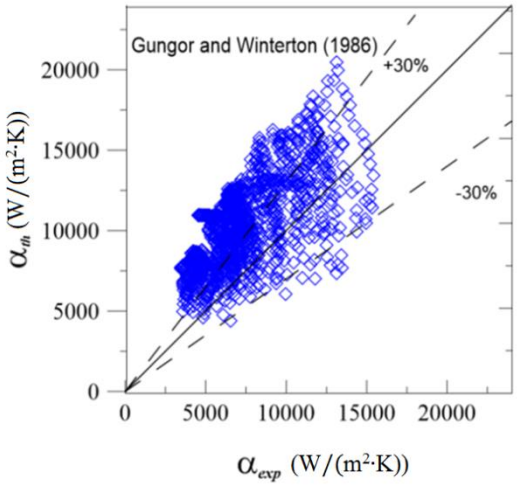

Figure 16. Comparison of the test results α_{exp} with predictions obtained α_{th} using the Gungor and Winterton (1986) correlation.

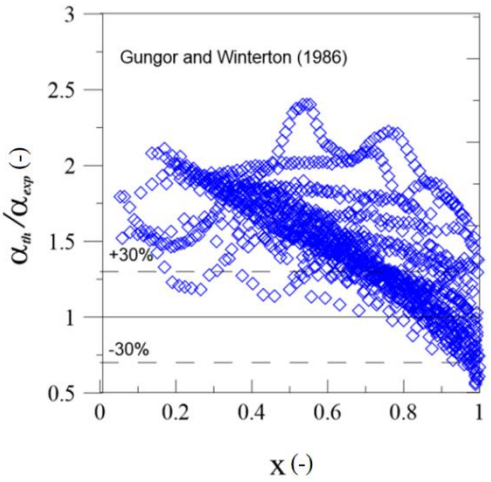

Figure 17. Comparison of the test results using the Gungor and Winterton (1986) correlation as a function of vapour quality.

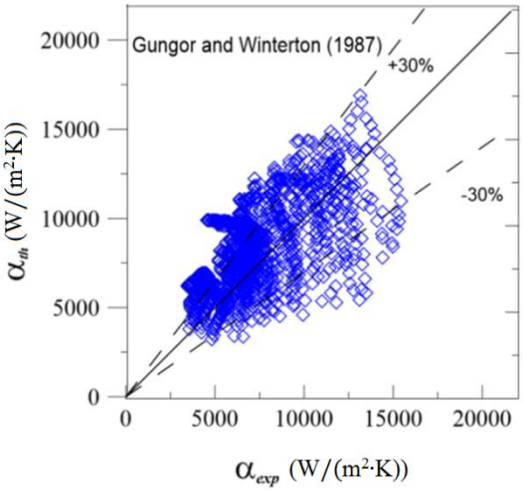

Figure 18. Comparison of the test results α_{exp} with predictions obtained α_{th} using the Gungor and Winterton (1987) correlation.

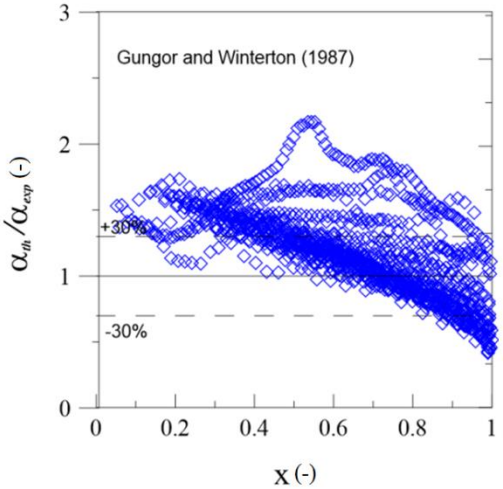

Figure 19. Comparison of the test results using the Gungor and Winterton (1987) correlation as a function of vapour quality.

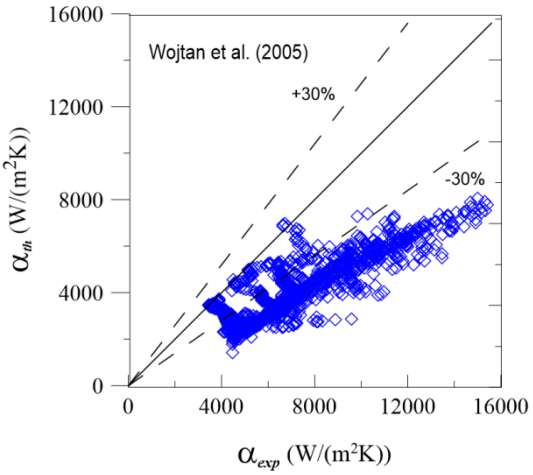

Figure 20. Comparison of the test results α_{exp} with predictions obtained α_{th} using the Wojtan et al. (2005) correlation.

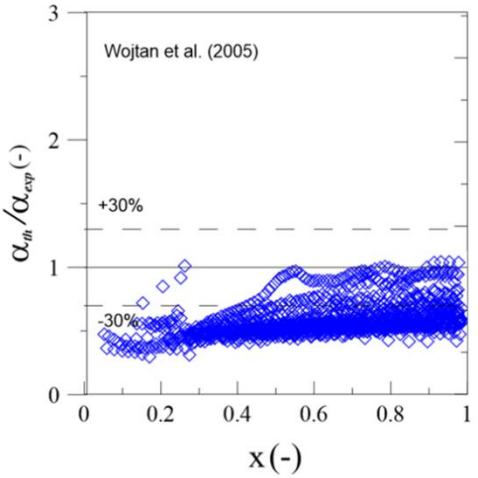

Figure 21. Comparison of the test results using the Wojtan et al. (2005) correlation as a function of vapour quality.

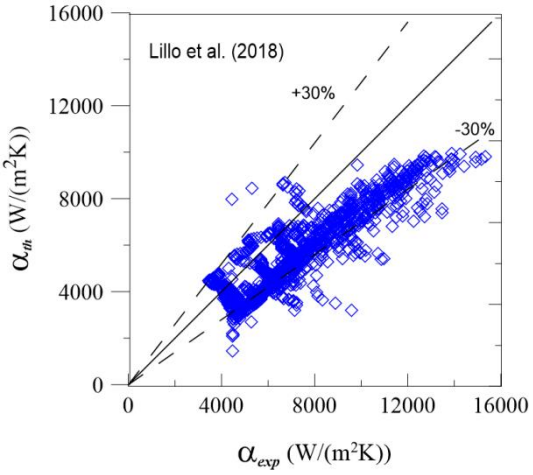

Figure 22. Comparison of the test results α_{exp} with predictions obtained α_{th} using the Lillo et al. (2018) correlation.

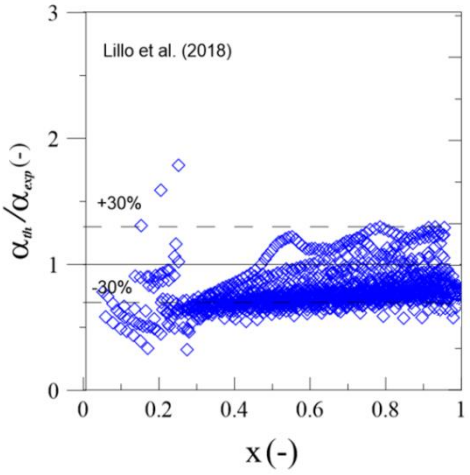

Figure 23. Comparison of the test results using the Lillo et al. (2018) correlation as a function of vapour quality.

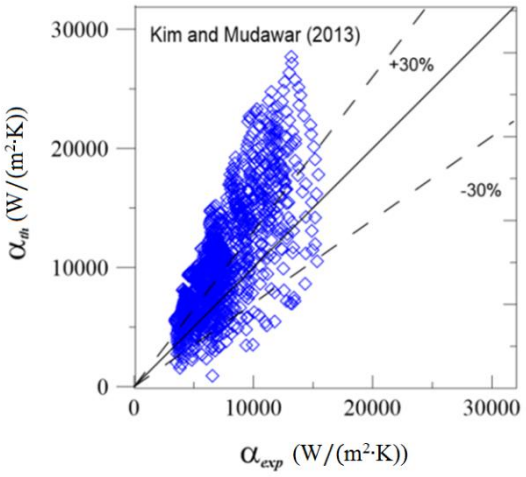

Figure 24. Comparison of the test results α_{exp} with predictions obtained α_{th} using the Kim and Mudawar (2013) correlation.

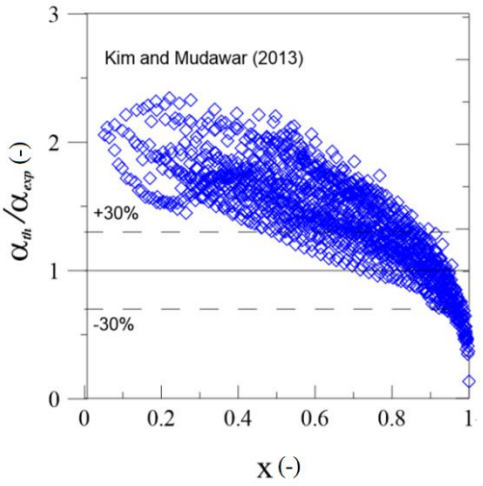

Figure 25. Comparison of the test results using the Kim and Mudawar (2013) correlation as a function of vapour quality.

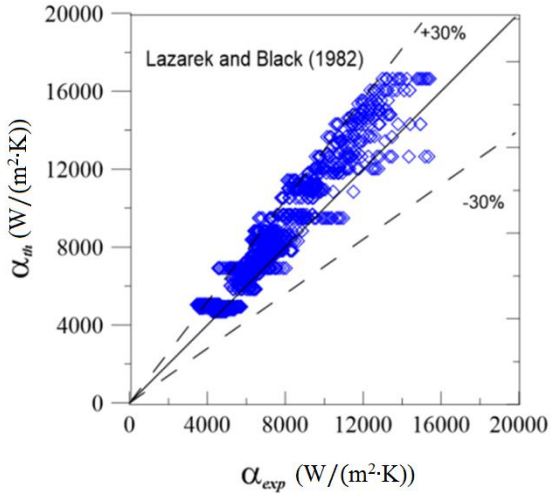

Figure 26. Comparison of the test results α_{exp} with predictions obtained α_{th} using the Lazarek and Black (1982) correlation.

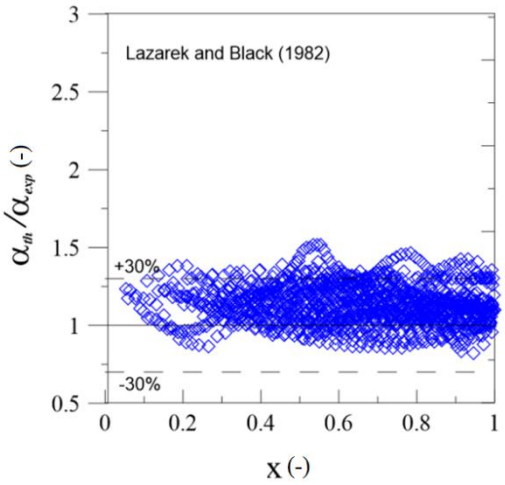

Figure 27. Comparison of the test results using the Lazarek and Black (1982) correlation as a function of vapour quality.

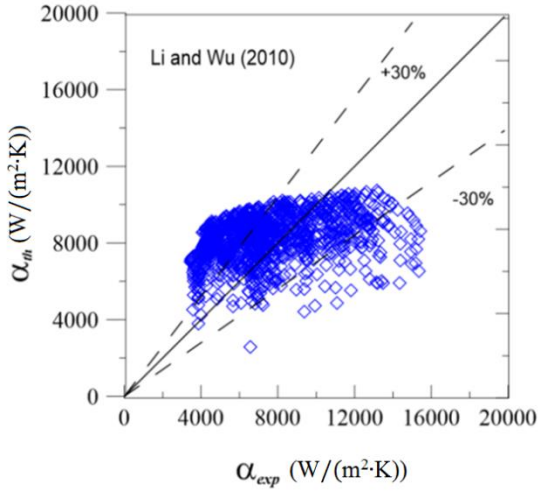

Figure 28. Comparison of the test results α_{exp} with predictions obtained α_{th} using the Li and Wu (2010) correlation.

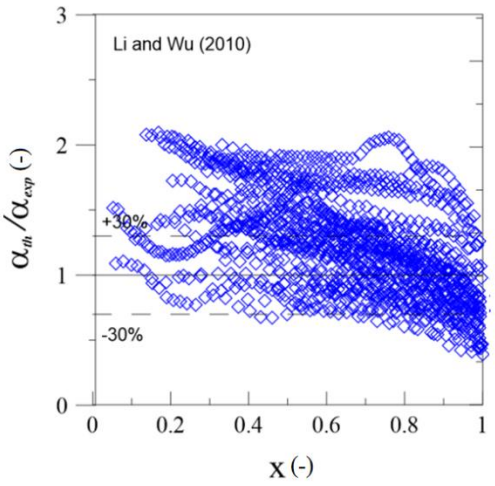

Figure 29. Comparison of the test results using the Li and Wu (2010) correlation as a function of vapour quality.

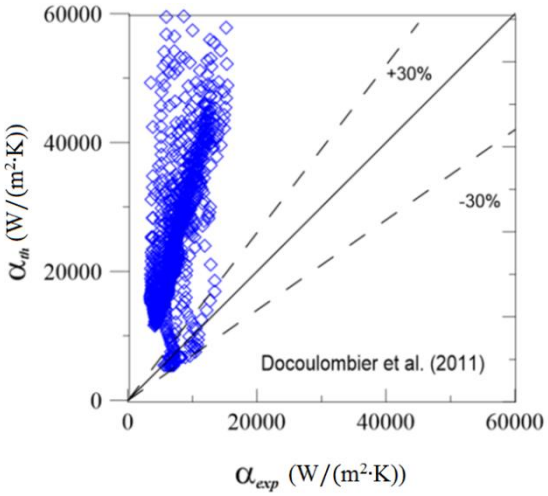

Figure 30. Comparison of the test results α_{exp} with predictions obtained α_{th} using the Docoulombier et al. (2011) correlation.

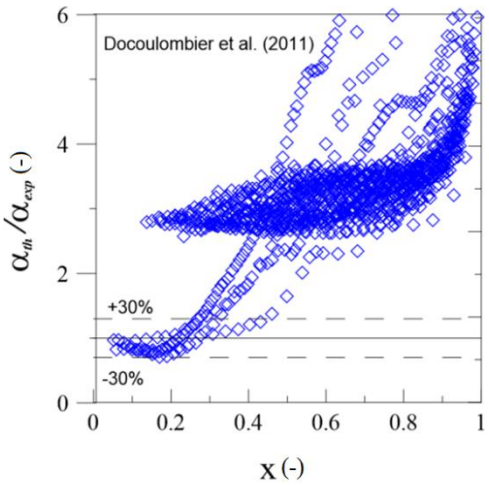

Figure 31. Comparison of the test results using the Docoulombier et al. (2011) correlation as a function of vapour quality.

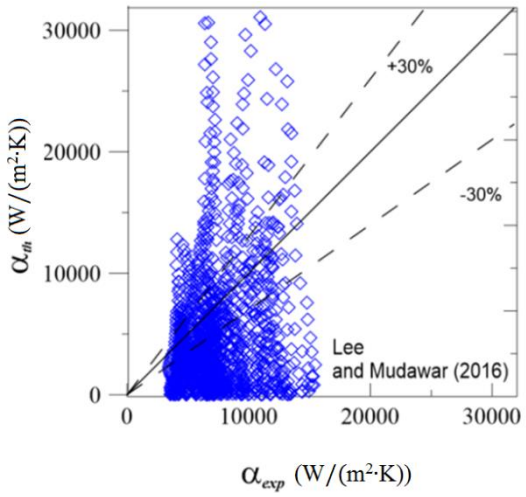

Figure 32. Comparison of the test results α_{exp} with predictions obtained α_{th} using the Lee and Mudawar (2016) correlation.

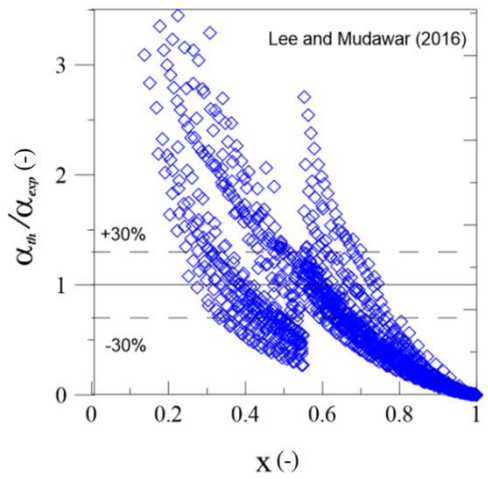

Figure 33. Comparison of the test results using the Lee and Mudawar (2016) correlation as a function of vapour quality.

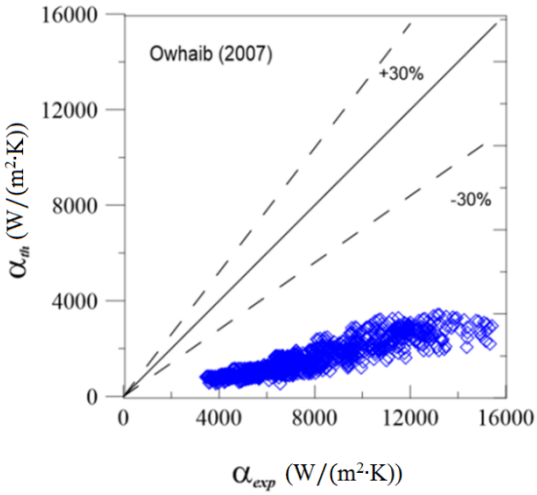

Figure 34. Comparison of the test results α_{exp} with predictions obtained α_{th} using the Owhaib (2007) correlation.

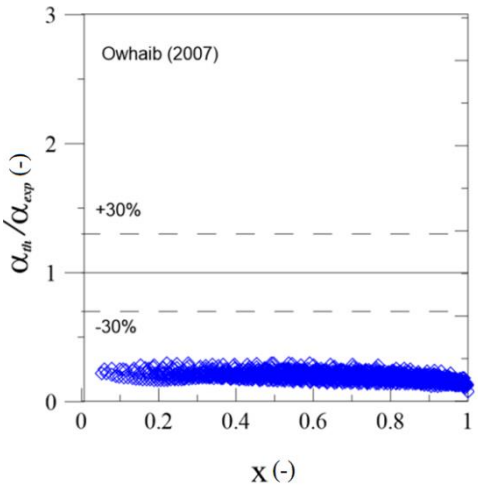

Figure 35. Comparison of the test results using the Owhaib (2007) correlation as a function of vapour quality.

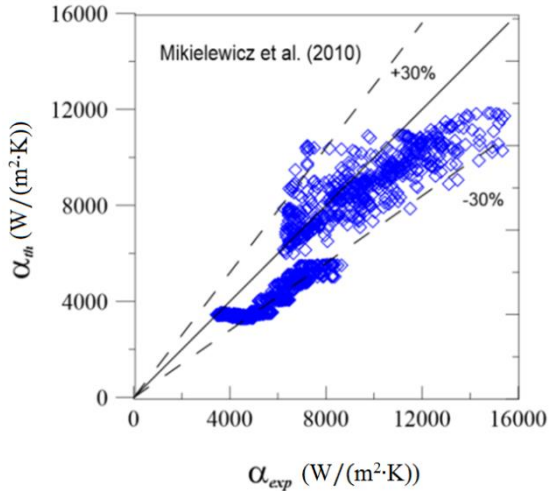

Figure 36. Comparison of the test results α_{exp} with predictions obtained α_{th} using Mikielewicz et al. (2010) correlation.

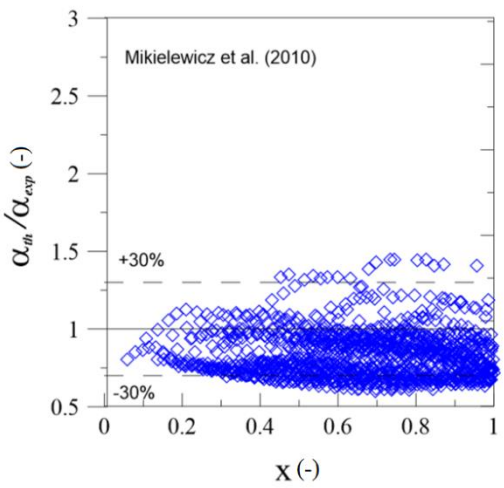

Figure 37. Comparison of the test results using the Mikielewicz et al. (2010) correlation as a function of vapour quality.

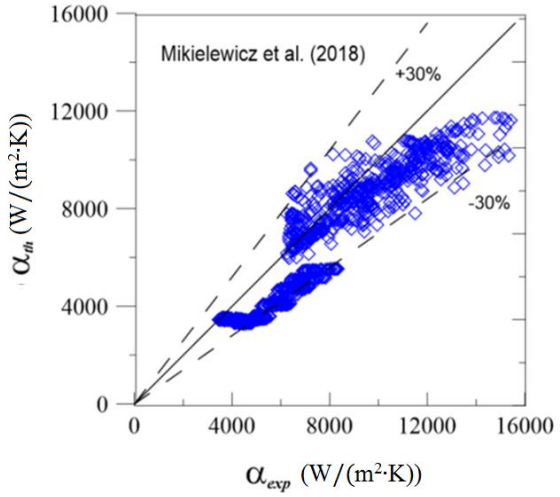

Figure 38. Comparison of the test results α_{exp} with predictions obtained α_{th} using the Mikielewicz et al. (2018) correlation.

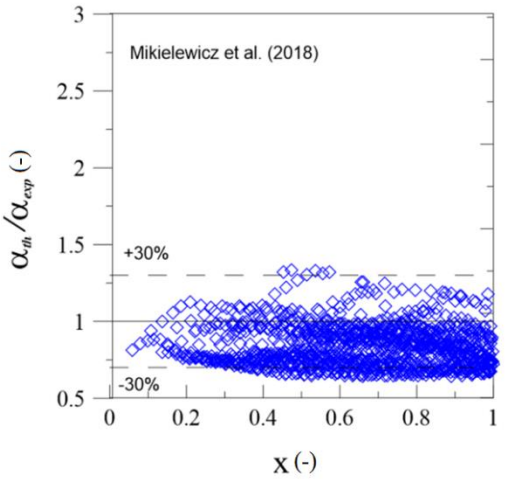

Figure 39. Comparison of the test results using the Mikielewicz et al. (2018) correlation as a function of vapour quality.

As can be seen according to presented figures the correlations due to Fang et al. (2017), Bertsch et al. (2009), Docoulmbier et al. (2011), Lee and Mudawar (2016) and Owhaib (2007) do not return satisfactory results of heat transfer coefficient predictions during flow boiling in the case of HFE7000. Moreover, the correlation due to Docoulmbier et al. (2011) gives the mean absolute deviation (*MAD*) greater than 100% and in the case of the correlation due to Owhaib (2007), there is no data within a ±30% error band. In fact, various studies such as those of Thome et al. [51], Bertsch et al. [36] and Cheng et al. [52], have reported that most of the existing heat transfer coefficient correlations, especially in the case for minichannel, were

developed based on a specific range of testing conditions. Hence, these correlations mostly show high deviations for the data beyond their often-narrow operating range [53].

Table 5 presents the values of mean absolute deviation (*MAD*) and the amount of experimental data within the error band of $\pm 30\%$ ($\eta_{\pm 30\%}$) for all investigated correlations. According to the comparisons presented in Figures 8–39, the calculation results obtained using the correlations due to Chen (1966), Lazarek and Black (1982), Shah (1976), Gungor and Winterton (1987) and Mikielewicz et al. (2010) and (2018) are satisfactory. Additionally, it should be noted that the correlation due to Mikielewicz et al. (2018), taking into account the effects of reduced pressure, is characterised by the smallest mean absolute deviation (*MAD* = 13.12%). Furthermore, the correlation due to Lazarek and Black (1982) is the second model with the lowest mean absolute deviation (*MAD* = 15.05%). In addition, the amount of data within the $\pm 30\%$ error is lower than in the case of both the original (2010) and modified Mikielewicz et al. (2018) models. While, as can be seen, the modified Mikielewicz et al. (2018) correlation gives a smaller *MAD* and greater $\eta_{\pm 30\%}$ than the original model.

Table 5. Statistical parameters from the comparison between the present experimental data and the prediction method.

Authors	*MAD*, %	$\eta_{\pm 30\%}$, %
Fang et al. [35]	54.90	9.94
Chen [32]	29.20	70.58
Bertsch et al. [36]	46.63	25.55
Shah [37]	27.31	66.56
Gungor and Winterton [38]	50.30	31.47
Gungor and Winterton [39]	29.47	58.26
Kim and Mudawar [40]	47.78	33.03
Wojtan et al. [41]	41.81	15.40
Lillo et al. [42]	24.55	77.53
Lazarek and Black [43]	15.05	89.97
Li and Wu [44]	35.30	53.57
Docoulombier et al. [45]	> 100	4.44
Lee and Mudawar [46]	71.10	25.31
Owhaib [47]	80.36	0.00
Mikielewicz et al. [30]	19.70	91.21

Mikielewicz et al. [20,48]	13.12	92.11

Mikielewicz et al.'s (2018) model is not the only one taking into account the effect of reduced pressure. Four other models examined, i.e. due to Fang et al. (2017), Kim and Mudawar (2013), Docoulombier et al. (2011) and Owhaib (2007), also take into account the effect of reduced pressure. However, these models do not return satisfactory predictive agreements with the experimental data in the case of HFE7000.

5. Conclusions

In this paper, an experimental study of the flow boiling heat transfer coefficients of HFE7000 in a vertical tube of 2.3 mm inner diameter in various operating conditions such as heat flux, saturated temperature, mass flux as well as vapour quality have been presented. Experiments have been carried out to identify the effects of heat flux, mass flux and saturation temperature on their influence of the flow boiling heat transfer coefficients. For this purpose, various operating conditions have been analysed in this study. While trying to capture as much as possible, the changes of parameters, which can be achievable to obtain at the presented experimental facility in case of HFE7000 flow boiling. Some characteristics and experimental data of HFE7000 flow boiling heat transfer in vertical tubes have been supplemented. The experimental data have been compared with some predictive methods from the literature. It is of great significance for the design of systems and devices using the HFE7000 refrigerant especially when the experimental research on the two-phase flow of this working fluid is still limited. The main conclusions of the present study are as follows:

1. The flow boiling heat transfer coefficient increases with increasing mass flux. However, the effect of increasing mass flux is less obvious and almost negligible on heat transfer coefficients.
2. As the saturated temperature goes up, the flow boiling heat transfer coefficient increases.
3. The flow boiling heat transfer coefficient increases significantly with the increasing heat flux, which is considered to be a dominating factor of the flow boiling heat transfer coefficient.
4. The heat transfer coefficient, initially, slightly decreases with vapour quality in the low-quality region and then increases with the further increase in vapour quality.
5. After the heat transfer coefficient reaches the maximum value, it decreases as the vapour quality goes up to a high vapour quality region.

6. The experimental data have been compared with 16 chosen correlations.
7. Among several chosen predictive models, the correlations due to Lazarek and Black and the semi-empirical in-house model due to Mikielewicz et al., with and without taking into account the effects of the reduced pressure, predict HFE7000 flowing boiling heat transfer coefficients satisfactorily.
8. Both correlations due to Mikielewicz et al. (2010) and (2018) give the greatest amount of experimental data within the error band of $\pm$30%.

Acknowledgements

Results presented in the paper have been funded from the project 2017/25/B/ST8/00755 by the National Science Centre, Poland.

Bibliography

[1] O. Evans, The Abortion of a Young Steam Engineer's Guide, Philadelphia, USA, 1805.

[2] J.M. Calm, The next generation of refrigerants – Historical review , considerations , and outlook, 31 (2008) 1123–1133. doi:10.1016/j.ijrefrig.2008.01.013.

[3] J. Perkins, Apparatus for producing ice and cooling fluids, 6662, 1834.

[4] R.C. Downing, History of the organic fluorine industry, second edi, John Wiley and Sons, Incoeporated, New York, USA, 1966.

[5] R.C. Downing, Development of chlorofluoro-carbon refrigerants, in: ASHRAE Trans. Am. Soc. Heating, Refrig. Air-Conditioning Eng., Atlanta, USA, 1984: pp. 481–491.

[6] United Nations, Final act of the conference of plenipotentiares on the proctection of the oznone, Vienna, 1985.

[7] United Nations Environment Program (UNEP), Montreal Protocol on Substances that Deplete the Ozone Layer (Final Act. United Nations), Montreal, 1987.

[8] United Nations Framework Convention on Climate Change (UNFCCC), Report of the Conference of the Parties, Kyoto, 1997.

[9] M.H. Rausch, L. Kretschmer, S. Will, A. Leipertz, A.P. Fröba, Density, Surface Tension, and Kinematic Viscosity of Hydrofluoroethers HFE-7000, HFE-7100, HFE-7200, HFE-7300, and HFE-7500, J. Chem. Eng. 60 (2015) 3759–3765. doi:10.1021/acs.jced.5b00691.

[10] A. Sekiya, S. Misaki, The Potential of Hydrofluoroethers to Replace CFCs, HCFCs and PFCs., J. Fluor. Chem. 101 (2000) 215–221. doi:10.1016/S0022-1139(99)00162-1.

[11] M. Ghodbane, An investigation of R152a and hydrocarbon refrigerants in mobile air conditioning, in: Int. Proc. Int. Congr. Expo., Warrendale, PA: SAE, Detroit, 1999: p. no. 1999-01-0874.

[12] B. Minor, M. Spatz, HFO-1234yf low GWP refrigerant update, in: Int. Int. Refrig. Air Cond. Conf. Purdue, West Lafayette, IN, USA, 2008: p. Paper no 2349.

[13] M.-C. Lu, J.-R. Tong, W. C-C, Investigation of the two-phase convective boiling of HFO-1234yf in a 3.9 mm diameter tube, Int. J. Heat Mass Transf. 65 (2013) 545–551. doi:10.1016/j.ijheatmasstransfer.2013.06.004.

[14] D. Del Col, S. Bortolini, D. Torresin, A. Cavallini, Flow boiling of R1234yf in a 1 mm diameter channel, in: Procedings 23rd IIR Int. Congr. Refrig., Prague, Czech Republic, 2011.

[15] D. Mikielewicz, J. Mikielewicz, J. Tesmar, Improved semi-empirical method for determination of heat transfer coefficient in flow boiling in conventional and small diameter tubes, Int. J. Heat Mass Transf. 50 (2007) 3949–3956. doi:10.1016/j.ijheatmasstransfer.2007.01.024.

[16] D. Mikielewicz, R. Andrzejczyk, B. Jakubowska, J. Mikielewicz, Analytical Model With Nonadiabatic Effects for Pressure Drop and Heat Transfer During Boiling and Condensation Flows in Conventional Channels and Minichannels, Heat Transf. Eng. 37 (2016) 1158–1171. doi:10.1080/01457632.2015.1112213.

[17] D. Mikielewicz, B. Jakubowska, Calculation method for flow boiling and flow condensation of R134a and R1234yf in conventional and small diameter channels, Polish Marit. Res. 24 (2017) 141–148. doi:10.1515/pomr-2017-0032.

[18] G. Lorentzen, Revival of carbon dioxide as refrigerant, Int. J. Refrig. 17 (1994) 292–301. doi:10.1016/0140-7007(94)90059-0.

[19] D. Mikielewicz, B. Jakubowska, Prediction of flow boiling heat transfer coefficient for carbon dioxide in minichannels and conventional channels, Arch. Thermodyn. 37 (2016) 89–106. doi:10.1515/aoter-2016-0014.

[20] D. Mikielewicz, B. Jakubowska, The effect of reduced pressure on carbon dioxide flow boiling heat transfer in minichannels, E3S Web Conf. 70 (2018). doi:10.1051/e3sconf/20187002012.

[21] Y. Zhao, Y. Liang, Y. Sun, C. J., Development of a mini-channel evaporator model using R1234yf as working fluid, Int. J. Refrig. 35 (2012) 2166–2178.

doi:10.1016/j.ijrefrig.2012.08.026.

[22] I. Bravo, Y. Díaz-de-Mera, A. Aranda, K. Smith, K.P. Shine, G. Marston, Atmospheric Chemistry of C4F9OC2H5 (HFE-7200), C4F9OCH3 (HFE-7100), C3F7OCH3 (HFE-7000) and C3F7CH2OH: Temperature Dependence of the Kinetics of Their Reactions with OH Figure 2. Liquid kinematic viscosity of HFEs under saturation conditions as a function, Phys.Chem. Chem. Phys. 12 (2010) 5115–5125. doi:10.1039/b923092k.

[23] W.-T. Tsai, Environmental Risk Assessment of Hydrofluoroethers (HFEs), J. Hazard. Mater. A119 (2005) 69–78. doi:10.1016/j.jhazmat.2004.12.018.

[24] 3M ™ Novec ™ 7000 Engineered Fluid, (n.d.) 1–6. https://multimedia.3m.com/mws/media/121372O/3m-novec-7000-engineered-fluid-tds.pdf.

[25] D. Mikielewicz, J. Wajs, R. Andrzejczyk, M. Klugmann, Pressure drop of HFE7000 and HFE7100 during flow condensation in minichannels, Int. J. Refrig. 68 (2016) 226–241. doi:10.1016/j.ijrefrig.2016.03.005.

[26] E.W. Lemmon, M.L. Huber, M.O. McLinden, NIST Standard Reference Database 23: Reference Fluid Thermodynamic and Transport Properties-REFPROP, Version 9.1, (2013).

[27] T. Muszyński, R. Andrzejczyk, B. Jakubowska, The impact of environmentally friendly refrigerants on heat pump efficiency, J. Power Technol. 99 (2019) 40–48.

[28] J. Wajs, D. Mikielewicz, B. Jakubowska, Performance of the domestic micro ORC equipped with the shell-and-tube condenser with minichannels, Energy. 157 (2018) 853–861. doi:10.1016/j.energy.2018.05.174.

[29] B.M. Fronk, S. Garimella, Measurement of heat transfer and pressure drop during condensation of carbon dioxide in microscale geometries, in: Proc. Int. Heat Transf. Conf., August 8–13, Washington, DC, 2010.

[30] D. Mikielewicz, A new method for determination of flow boiling heat transfer coefficient in conventional diameter channels and minichannels, Heat Transf. Eng. 31 (2010) 276–287. doi:10.1080/01457630903311694.

[31] M. Eraghubi, P. Di Marco, A.J. Robinson, Low mass flux upward vertical forced flow boiling of HFE7000, Exp. Therm. Fluid Sci. 102 (2019) 291–301. doi:10.1016/j.expthermflusci.2018.11.011.

[32] J.C. Chen, Correlation for boiling heat transfer to saturated fluids in convective flow, Ind. Eng. Chem. Process Des. Dev. 5 (1966) 322–329. doi:10.1021/i260019a023.

[33] R.J. Moffat, Describing the uncertainity in experimental results, Exp. Therm. Fluid Sci.

1 (1985) 3–17. doi:10.1016/0894-1777(88)90043-X.

[34] J.B. Copetti, M.H. Macaganan, F. Zinani, Experimental study on R-600a boiling in 2.6 mm tube, Int. J. Refrig. 36 (2013) 325–334. doi:10.1016/j.ijrefrig.2012.09.007.

[35] X. Fang, Q. Wu, Y. Yuan, A general correlation for saturated flow boiling heat transfer in channels of various sizes and flow directions, Int. J. Heat Mass Transf. 107 (2017) 972–981. doi:10.1016/j.ijheatmasstransfer.2016.10.125.

[36] S.S. Bertsch, E.A. Groll, S. V. Garimella, A composite heat transfer correlation for saturated flow boiling in small channels, Int. J. Heat Mass Transf. 52 (2009) 2110–2118. doi:10.1016/j.ijheatmasstransfer.2008.10.022.

[37] M. Shah, A new correlation for heat transfer during boiling flow through pipes, ASHRAE Trans. Tom. II (1976) 66–86.

[38] K.E. Gungor, R.H.S. Winterton, A general correlation for flow boiling in tubes and annuli, Int. J. Heat Mass Transf. 29 (1986) 351–358. doi:10.1016/0017-9310(86)90205-X.

[39] K.E. Gungor, R.H.S. Winterton, Simplified general correlation for saturated flow boiling and comparisons of correlations with data, Chem. Eng. Res. Des. 65 (1987) 148–156.

[40] S.M. Kim, I. Mudawar, Universal approach to predicting saturated flow boiling heat transfer in mini/micro-channels - Part II. Two-phase heat transfer coefficient, Int. J. Heat Mass Transf. 64 (2013) 1239–1256. doi:10.1016/j.ijheatmasstransfer.2013.04.014.

[41] L. Wojtan, T. Ursenbacher, J.R. Thome, Investigation of flow boiling in horizontal tubes: Part II—Development of a new heat transfer model for stratified-wavy, dryout and mist flow regimes, Int. J. Heat Mass Transf. 48 (2005) 2970–2985. doi:10.1016/j.ijheatmasstransfer.2004.12.013.

[42] G. Lillo, R. Mastrullo, A.W. Mauro, L. Viscito, Flow boiling heat transfer, dry-out vapor quality and pressure drop of propane (R290): Experiments and assessment of predictive methods, Int. J. Heat Mass Transf. 126 (2018) 1236–1252. doi:10.1016/j.ijheatmasstransfer.2018.06.069.

[43] G.M. Lazarek, S.H. Black, Evaporative heat transfer pressure drop and critical heat flux in a small vertical tube with R-113, Int. J. Heat Mass Transf. 25 (1982) 945–960. doi:10.1016/0017-9310(82)90070-9.

[44] W. Li, Z. Wu, A general correlation for evaporative heat transfer in micro/mini-channels, Int. J. Heat Mass Transf. 53 (2010) 1778–1787.

doi:10.1016/j.ijheatmasstransfer.2010.01.012.

[45] M. Docoulombier, S. Colasson, B. J., P. Haberschill, Carbon dioxide flow boiling in a single microchannel – Part II: Heat transfer, Exp. Therm. Fluid Sci. 35 (2011) 597 – 611. doi:10.1016/j.expthermflusci.2010.11.014.

[46] S. Lee, I. Mudawar, Investigation of flow boiling in large micro-channel heat exchangers in a refrigeration loop for space applications, Int. J. Heat Mass Transf. 97 (2016) 110–129. doi:10.1016/j.ijheatmasstransfer.2016.01.072.

[47] W. Owhaib, Experimental Heat Transfer , Pressure Drop , and Flow Visualization of R-134a in Vertical Mini / Micro Tubes, KTH, School of Industrial Engineering and Management (ITM), 2007.

[48] D. Mikielewicz, B. Jakubowska, Comparison of predictive methods for flow boiling heat transfer in conventional channels and minichannels - the effect of reduced pressure, MATEC Web Conf. 240 (2018). doi:10.1051/matecconf/201824001028.

[49] J. Mikielewicz, Semi-empirical method of determining the heat transfer coefficient for subcooled staurated boiling in a channel, Int. J. Heat Transf. 17 (1973) 1129–1134. doi:10.1016/0017-9310(74)90114-8.

[50] P.A. Kew, K. Cornwell, Correlations for the prediction of boiling heat transfer in small diameter channels, Appl. Therm. Eng. 17 (1997) 705–715. doi:https://doi.org/10.1016/S1359-4311(96)00071-3.

[51] J.R. Thome, Boiling in microchannels: a review of experiment and theory, Int. J. Heat Fluid Flow. 25 (2004) 128–139. doi:10.1016/j.ijheatfluidflow.2003.11.005.

[52] L. Cheng, Fundamental issues of critical heat flux phenomena during flow boiling in microscale-channels and nucleate pool boiling in confined spaces, Heat Transf. Eng. 34 (2013) 1011–1043. doi:10.1080/01457632.2013.763538.

[53] N. Chien, K. Choi, J.-T. Oh, H. Cho, An experimental investigation of flow boiling heat transfer coefficient and pressure drop of R410A in various minichannel multiport tubes, Int. J. Heat Mass Transf. 127 (2018) 675–686. doi:10.1016/j.ijheatmasstransfer.2018.06.145.